합성형교량의 설계온도하중

Design Thermal Loads In Composite Box Girder Bridges

장 승 필[1] · 임 창 균[2]

Chang, Sung Pil *Im, Chang Kyun*

요 약 : 본 논문에서는 장기온도측정자료의 통계해석에 바탕을 두고, 합성박스형교량에 작용하는 설계온도하중의 적절한 값을 제안하고자 한다. 이를 위해, 최근에 건설된 합성박스형교량에서 약 20개월간 온도측정을 수행하였다. 극치해석에 앞서, 온도분포특성을 나타내는 주요 매개변수를 정의하고, 이의 계절별변화에 대해 상세히 검토하였다. 이 온도하중매개변수의 극치분포를 Tail-Equivalence법에 의해 결정하고, 주어진 재현기간에 해당되는 온도하중매개변수의 극치값을 계산하였다. 끝으로, 이 결과들을 현 시방서에서 온도하중에 대해 제안하고있는 규정들과 비교하였다. 비교결과로부터, 현 시방서는 합성박스형교량의 온도응력을 나타내는데 불충분하며, 특별한 경우에 있어서 현 설계규정에 포함되지않은 수평방향온도변화를 고려해야만 된다는 결론에 도달하였다.

ABSTRACT : The intention of this paper is to provide realistic values of design thermal loads applicable to composite box girder bridges on the basis of the statistical analysis of long-term measured temperature data. For this purpose, temperatures were recorded at a newly constructed composite box girder bridge during about 20 months. Before analyzing the extreme values, major thermal loading parameters that characterize the temperature profile are defined, and a seasonal behavior of those is examined in detail. The limit distributions of the thermal loading parameters are then determined by the tail-equivalence method, and the thermal loading parameters corresponding to selected return period are calculated. Finally, the results are compared to the specifications suggested in a current design code for thermal loads, and it is concluded that the current design code is unsuitable for representing the self-equilibrated thermal stresses in composite bridges, and the horizontal temperature difference which is not suggested in current design code should be taken into account in particular cases.

핵 심 용 어 : 온도하중매개변수, 환경온도영향, 합성박스형교량, Tail-equivalence법.

KEYWORDS : thermal loading parameters, environmental thermal effects, composite box girder bridge, tail-equivalence method.

1) 정회원, 서울대학교 토목공학과교수

2) 서울대학교 토목공학과 박사수료

본 논문에 대한 토의를 1999년 3월 31일까지 학회로 보내주시면 토의 회답을 게재하겠습니다.

1. Introduction

The development of thermal loading criteria for design on bridge subjected to environmental thermal effects has recently received considerable attention.[1,2,3]

Unfortunately, the environmental condition upon which temperature profile in bridge depends exhibits variation with successive years as well as days and the seasons. Therefore, thermal loads which are subjected to such variables should be considered as random variables and rational conclusions with regard to the thermal loads can only be obtained based on statistical analysis.

Researches on the extreme analysis of environmental loads in offshore structure[4] and of snow loads using local climatological data[5] have been carried out, and several authors[1,2,3] have carried out researches on the extreme thermal loads in concrete bridges to environmental thermal effects. On the other hand, there is not any suggestion on the design criteria or extreme values of thermal loads for composite box girder bridges, although several studies[6,7,8] have shown the thermal effects in composite box girder bridges subjected to environmental thermal conditions by analytical or experimental investigations.

Therefore, this paper intends to present the procedure of developing thermal loading criteria in composite steel box girder bridges for design on the basis of extreme value analysis. For the purpose, an experimental investigation was conducted to obtain temperature data on a composite bridge for a period from September 1996 to April 1998 which allows for the full seasonal cycle, and the parameters of thermal loads which describe the thermal response of bridges are identified and are investigated for the seasonal behavior in detail. In the extreme value analysis, the tail-equivalence method which is described in Maes et al.(3) is used to determine the limit distribution from which the values of the thermal loading parameters with selected return period are calculated. Finally the computed extreme values are compared to those suggested in current design specifications for thermal loads.

2. Experimental Instrumentation

Site measurements of temperatures have been carried out on a composite box-girder viaduct located at the south of Seoul to perform the study of previously mentioned statistical analysis. The viaduct shown in Fig. 1, 300m long, consists of six spans with span length 50m and is

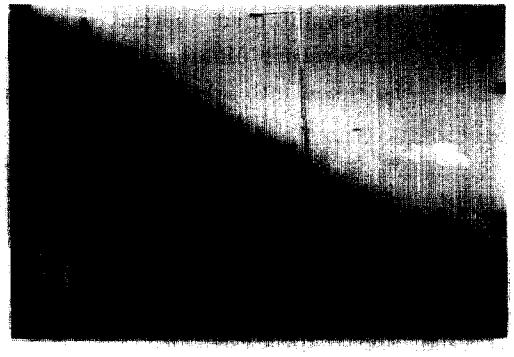

Fig. 1 Sa-Dang Viaduct

made up of steel-concrete composite box girder with depths varying from 2.35m at the pier supports to 1.845m at mid-span. The superstructure is made of parallel two separate decks constructed with two composite box girders(see Fig. 2(a)). The slightly curved viaduct axis is generally in a East-West direction.

One cross-section of the viaduct within the second span from the west end was selected for temperature measurement. When the viaduct was under construction, 30 copper-constant thermocouples were installed in the concrete slab as well as on the interior surface of steel girder of the cross section. The thermocouples were installed only in the southern box girder, since it is difficult to measure the temperatures everywhere within the cross section made up of four box girders. To consider the effects of the difference in exposure condition to direct solar radiation, thermocouples were located on both side webs of the southern box girder in an attempt to record any differences in horizontal direction. The position of thermocouples and their numbering sequence are illustrated in Fig. 2(b).

The environmental thermal loads on bridges vary with the seasons as well as daily, so it is required for the temperatures to be recorded during a year or more. In this study the temperature measurement, therefore, has been conducted over a 20-month period. Although the first thermocouple reading was taken in September 1996 and the last reading was taken on April 1998 in hourly intervals,

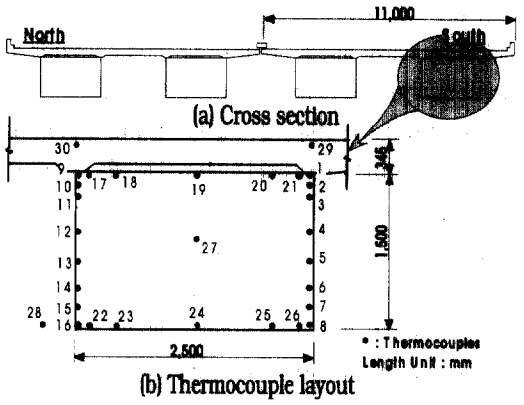

Fig. 2 Test section and thermocouple layout

because of system failures the temperature data for a period from April 1997 to April 1998 are used in this study.

3. Analysis Of Measured Data

3.1 Thermal Loading Parameters

Thermal load for design is not the variation of temperature at just one point in the bridge. It is, therefore, convenient to have key parameters that characterize the temperature profile and from which structural response can be determined.

Thus, this section represents the procedure of defining the thermal loading parameters on a composite girder section.

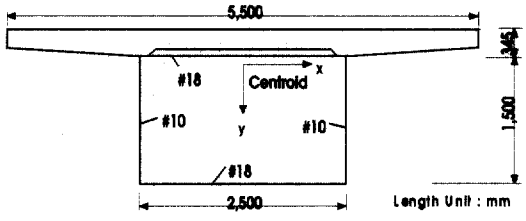

Fig. 3 Hypothetical cross section

Fig. 3 shows the hypothetical cross section composed of one cell box girder for which the thermal loading parameters are considered. It has exactly same geometry of the southern steel box girder of the test section(see Fig. 2) except that the concrete slab is slightly modified to have symmetric shape with width 5.5m and equal depth 0.345m over a web. Measured temperature profile at thermocouple nodes is regarded as the same that of the hypothetical cross section. It is based on the assumption that the concrete slab away from a web has only vertical heat flow, so the temperature profiles of any two girder sections are perfectly independent.

Under a temperature distribution, T the hypothetical cross section will attempt to obtain strain of αT where α is the linear coefficient of thermal expansion. The temperature distribution is not necessary to be uniform in horizontal direction of the cross section.

The free strain, αT of cross section can be then broken down into several strain components. According to the decomposition of the strain field, the measured temperature distribution on the cross section will be considered as three thermal loading parameters; namely, (i) the effective temperature T_e inducing axial movement, (ii) the differential temperature for vertical and horizontal respectively ΔT_v, ΔT_h inducing curvature, and (iii) the maximum and minimum values of self-equilibrated stresses in the cross section, $\sigma_{s,\max}$ and $\sigma_{s,\min}$ respectively. Then, the thermal loading parameters of measured data can be computed by simple summation over sub-areas which is contributed to each thermocouple node as shown in Eqs. (1) to (3) to follow. In this analysis, it is assumed that the linear coefficients of thermal expansion for concrete and steel are equal and the Euler-Bernoulli assumption that plane sections remain plane is valid.

$$T_e = \frac{\sum_i E_i T_i A_i}{\sum_i E_i A_i} \tag{1}$$

$$\Delta T_v = -D \frac{\sum_i E_i T_i \bar{y}_i A_i}{\sum_i E_i \bar{y}_i^2 A_i} \tag{2a}$$

$$\Delta T_h = -W \frac{\sum_i E_i T_i \bar{x}_i A_i}{\sum_i E_i \bar{x}_i^2 A_i} \tag{2b}$$

$$\sigma_{s,\max} = \max\{\sigma_{s,i}\} \tag{3a}$$

$$\sigma_{s,\min} = \min\{\sigma_{s,i}\} \tag{3b}$$

$$\sigma_{s,i} = E_i \alpha_i \left[T_e - \frac{\Delta T_v y_i}{D} - \frac{\Delta T_h x_i}{W} - T_i \right] \tag{4}$$

where,

i : each thermocouple node $(1 \le i \le 30)$,

T_i : measured temperature at thermocouple node i(see Fig. 2(b)),

A_i : each portion of cross-sectional area A contributed to thermocouple node i,

E_i : the modulus of elasticity for A_i,

α_i : the thermal expansion coefficient for A_i,

$\sigma_{s,i}$: self-equilibrated thermal stresses at thermocouple node i,

x_i, y_i : distance from centroid of the cross-section to thermocouple node i,

$\overline{x_i}, \overline{y_i}$: distance from centroid of the cross-section to centroid of sub-area A_i,

W : width of the cross-section,

D : depth of the cross-section.

3.2 Seasonal Behavior of the Thermal Loads

Before statistical analysis of data of the thermal loading parameters, it is worthwhile examining a seasonal behavior of the peak values of those. Figure 4 shows plots of the hourly data of previously defined thermal loading parameters. The data plotted had been measured during the period from April in 1997 to April in 1998, but due to the system failure some gaps in the readings occurred during several days of Jun, July and November. Thus, there are 310 days when all hourly temperature readings are complete.

A thorough examination of the peak values of hourly data of the thermal loading parameters shown in Fig. 4 reveals some interesting patterns. All of 30 T_e peaks for maximum, as expected, occurred between 15:00 and 17:00 just after maximum ambient air temperature occurs in summer months (June, July and Aug.), T_e peaks for minimum usually occurred just before and after dawn in winter months (Dec., Jan. and Feb.). During the period of measurement the extreme peak of T_e for maximum of 39.8℃ was recorded on 23 July 1997 and the extreme peak of T_e for minimum of -6.6℃ on 3 December 1997. The two extreme peaks of T_e and the extreme ambient air temperatures occur just on the same days, respectively.

Fig 4(b) shows the hourly variation of the vertical temperature differentials, ΔT_v defined in Eq.(2a). In the plot, a positive value indicates the top surface is hotter than the bottom flange, and vice versa. Generally speaking, it is much harder to detect trends for ΔT_v peaks than for the previous effective temperature. All the 30 ΔT_v peaks for maximum occurred during summer months except one. The peak values also have a tendency to occur over the entire time of a day, especially there are two peaks in the day followed by a sunny day. One is occurred after midnight and another is occurred during afternoon. It is supposed to be caused by the difference of thermal

material properties between concrete and steel, that is, after day time of the previous sunny day the temperature in steel is decreased faster than in concrete.

The cross section is subjected to a negative vertical temperature difference when the web of steel box girder is directly exposed to solar radiation. All the 30 ΔT_v peaks for minima which occurred during winter months are caused by the lower altitude of sun, moreover the magnitude is greater than that of the ΔT_v for maxima. During the period of measurement the extreme value of ΔT_v for maximum of 8.6℃ was recorded at 17:00 on 14 August 1997 and the extreme value of ΔT_v for minimum of -11.96℃ at 14:00 on 26 December 1997.

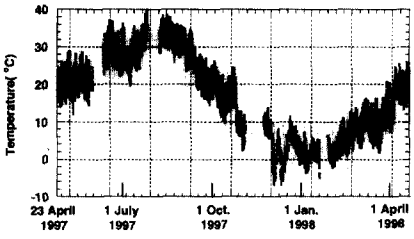

(a) Hourly variation of T_e

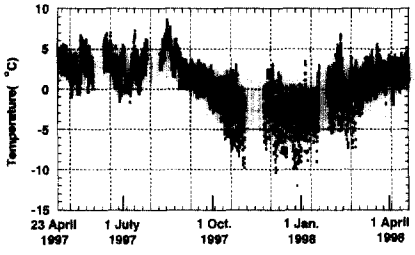

(b) Hourly variation of ΔT_v

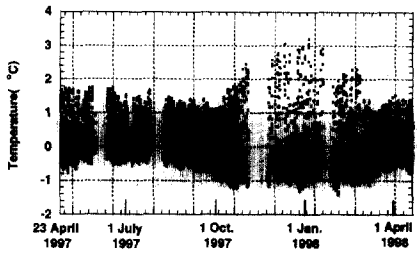

(c) Hourly variation of ΔT_h

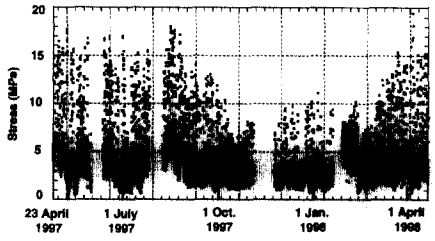

(d) Hourly variation of $\sigma_{s,\max}$

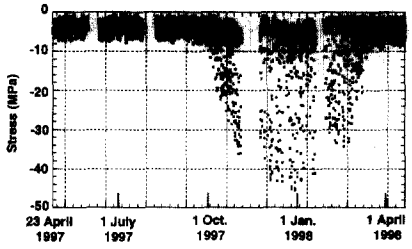

(e) Hourly variation of $\sigma_{s,\min}$

Fig. 4 Hourly variation of thermal loading parameters

The temperature distributions for these cases are plotted in Figs. 5(a) and 5(b). Figure 4(c) shows the hourly variation of the horizontal temperature differences which imposes horizontal thermal curvature. In this plot, a positive value, generally speaking, indicates the south

facing surface of the cross section is hotter than the north surfacing surface. It is reveals that the difference is no longer negligible. It is of the same order of magnitude as the vertical temperature differences in the winter months. During the period of measurement the extreme value of ΔT_h for maximum was recorded at 14:00 on 4 January 1998, and the temperature distributions at this time is plotted in Fig. 5(c).

Figure 4(d) and (e) show the hourly variation of maximum(tensile) an minimum (compressive) self-equilibrated stresses $\sigma_{s,\max}$, $\sigma_{s,\min}$ respectively, defined in Eq. (3). The 30 $\sigma_{s,\max}$ peaks for maximum entirely occurred between 14:00 and 16:00 in spring and summer months. All of the $\sigma_{s,\max}$ peaks occurred in the thermocouple node 21 (see Fig. 2) of the top flange close to north-facing web.

The $\sigma_{s,\min}$ peaks for minimum usually occurred at the same time during the day to indicate that may be influenced by the amount of strong direct solar radiation. All of the $\sigma_{s,\min}$ peaks occurred in the thermocouple node 6 or 7(see Fig. 2(b)) on the south-facing web during the winter months, and they occur entirely between 11:00 and 15:00, in which the maximum frequency of occurrence was recorded at 13:00. The patterns of occurrence can be explained by following. The lateral south-facing web of the box girder exposed to direct solar radiation undergoes a sizable temperature increase

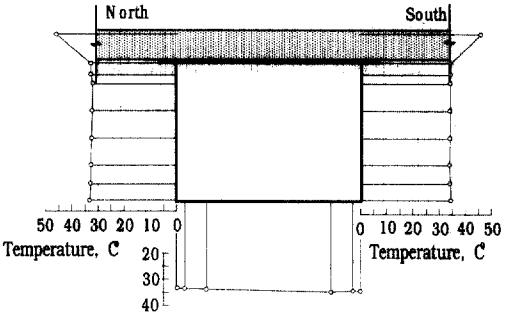

(a) Temperature distribution for the maximum value of ΔT_v

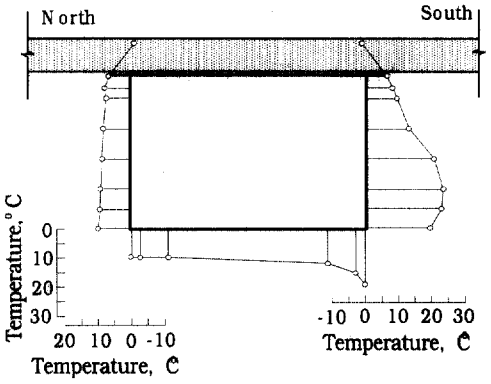

(b) Temperature distribution for the minimum value of ΔT_v

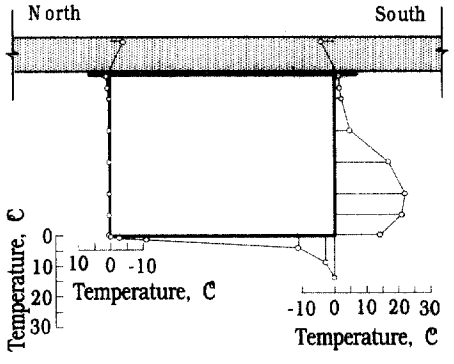

(c) Temperature distribution for the maximum value of ΔT_h

Fig. 5 Temperature distributions for maximum and minimum temperature differences

almost instantly.

The assumption of the Navier-Bernouilli hypothesis causes self-equilibrated thermal stress distributions to appear, so that the zone of the lateral surface exposed to direct solar radiation is subjected to large compressive stresses of a magnitude proportional to the global solar radiation acting on the lateral surface of the composite deck. In addition to these conditions, an overhanging cantilever slab provides shade on a lateral web of a bridge. The extreme value of $\sigma_{s,\min}$ is, therefore, occurred not in days of summer months, but in sunny days of winter months with lower solar altitude.

In order to illustrate the point above, Fig. 6 shows the distributions of self-equilibrated thermal stresses, σ_s defined in Eq. (4) with extreme tensile and extreme compressive values recorded during the period of measurement. This figure shows that the magnitude of the compressive stresses in the south-facing web of the box girder is quite different than that in the north-facing web. The maximum compressive stress in the box girder is 45.38MPa and take place at 13:00h. Similar results were presented by other authors.(7,8) Therefore, emphasis should be placed on the magnitude of the self-equilibrated compressive thermal stresses in the lateral web exposed to direct solar radiation.

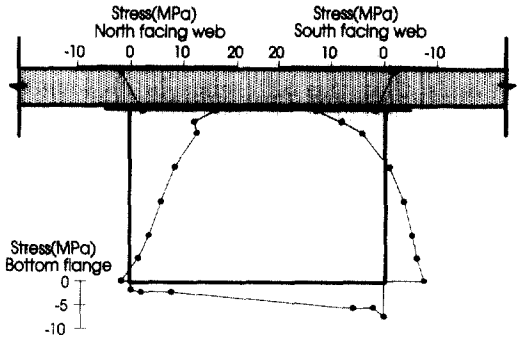

(15:00, 6 April, 1998)

(a) Stress profile with maximum value

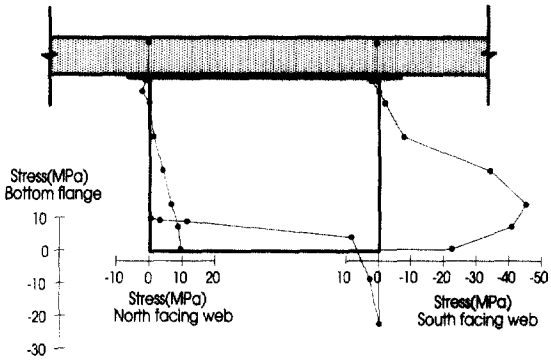

(13:00, 28 Dec., 1997)

(b) Stress profile with minimum value

Fig. 6 Self-equilibrated longitudinal stresses at thermocouple nodes

4. Design Values Of Thermal Loads

In the bridge design for thermal loads which show considerable variation over years, it is necessary to estimate the largest or smallest thermal loading parameter values that are likely to occur for a given return period. Therefore, consideration on the maximum values of measured data over a period of one or two years are not sufficient for design purpose, but further statistical analysis of

the result of measured temperature data is needed to determine the design values.

In this section an attempt is made to show how data of thermal loading parameters can be analyzed using extreme value theory. In order to accomplish this, it is necessary to determine the limiting distribution of the maximum (or minimum) of the data. Tail equivalence technique of the extreme value theory to problems of thermal loading parameters which is represented in Maes et al.(3), is considered to determine the type of the limiting distribution. With the known limiting distribution, the thermal loading parameters corresponding to a certain return period are to be calculated. Resnick(9) shows the clear connection between tail equivalence and domains of attraction. This has very important practical implications, because a distribution $F(x)$ can be replaced by a tail equivalent distribution $G(x)$ without altering either the domain of attraction or the set of admissible constants. If $G(x)$ is one of the three extreme value distribution: the Gumbel, the Frechet, or the Weibull distribution, the problem becomes considerably simpler. In other words, from a practical point of view, one of the three extreme value distribution can be fitted to the tail of a given distribution and use it for extreme value purposes(10), which is the basis for the method to be presented in this paper to estimate the thermal loading parameter with selected return periods.

The analysis begins with the identification of the peak values of the variables. Each variable $X(t)$ of thermal loading parameters is plotted against time t in Fig. 4, and the values of distinct peaks of the resulting plot are recorded. The actual number of peaks considered does not matter greatly, about $0.005\,n$ peaks should be identified(3), where n is the total number of data points.

In order to identify to which of the three extreme value tails the peak values of each of the empirical data sets of thermal loading parameters belong, Gumbel probability papers are used. The peaks X_i, ranked in increasing order of magnitude, are plotted against η_i, the double logarithm of their empirical cumulative distribution values p_i.

$$\eta_i = -\ln(-\ln p_i) \quad \text{(for minima)} \tag{5a}$$

$$\eta_i = \ln(-\ln(1-p_i)) \quad \text{(for minima)} \tag{5b}$$

where, $p_i = \dfrac{i}{n+1}$,

n : total number of data points,

i : ranking in increasing order of magnitude.

On Gumbel probability paper for largest (smallest) values, the Weibull distributions appear as convex (concave) curves, the Frechet distributions as concave (convex) curves, and the Gumbel distributions as straight line(10). This property is used in

testing the domain of attraction of the cumulative distribution function of the given data of thermal loading parameters. Fig. 7 shows the Gumbel plot of the thermal loading parameters.

According to observation on the Gumbel plot of Fig. 7, T_e for maxima and minima show a linear trend in all of its range, and it is assumed to follow a Gumbel distribution for maxima and minima, respectively. Also, the vertical temperature difference ΔT_v for maxima illustrates clear evidence that it comes from a Gumbel distribution for maxima.

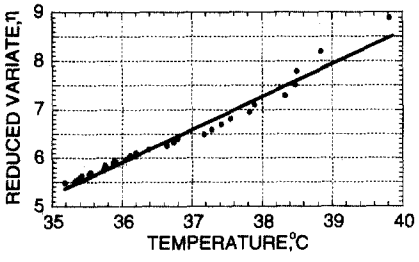

(a) Gumbel plot of T_e for maxima

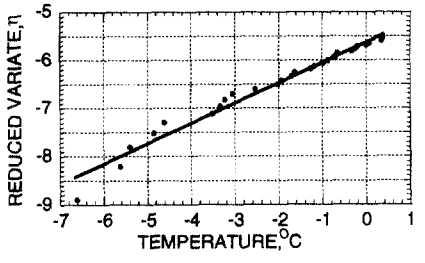

(b) Gumbel plot of T_e for minima

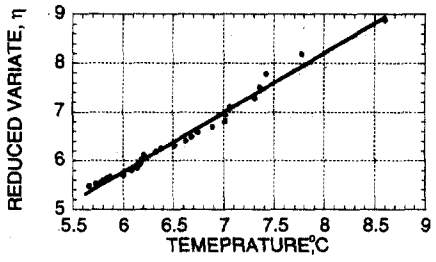

(c) Gumbel plot of ΔT_v for maxima

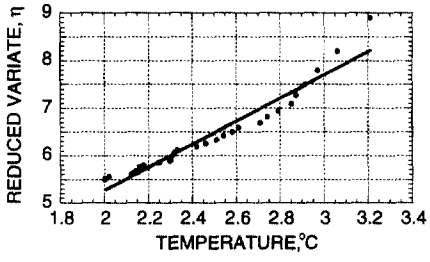

(d) Gumbel plot of ΔT_h for maxima

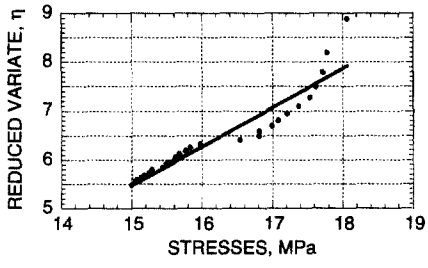

(e) Gumbel plot of $\sigma_{s,\max}$ for maxima

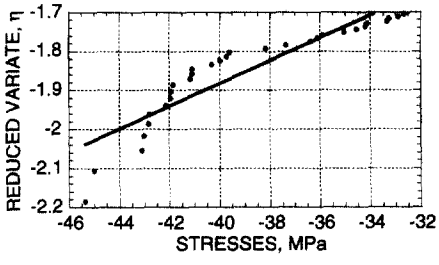

(f) Gumbel plot of $\sigma_{s,\min}$ for minima

Fig. 7 Gumbel plot of thermal loading parameters

On the other hand, the $\sigma_{s,\max}$ for maxima as well as ΔT_h for minima does not show a linear trend in its range, but a convex shape in right tail. Thus, this suggests a Weibull type limit distribution. And the $\sigma_{s,\min}$ for minima shows clear evidence that it does not come from a Gumbel distribution for minima. The curvature of the trend in the left tail suggests a Weibull distribution.

Subsequent to determining the type of the extreme distribution, the parameters of the extreme distribution which are the location parameter α and scale parameter β in Gumbel distribution and the location parameter λ and scale parameter δ and shape parameter γ in Weibull distribution, are estimated in the way of direct minimization in an iterative estimation procedure of E_r in Eq. (6). As the method for such calculation, the procedure developed by Fiacco and McCormick(11) is used. A rapid rate of convergence of many of the above iterative method depends upon a good initial estimate of the parameters.

$$E_r = \sum_{i=j}^{k} W_i [F(x_i;\theta) - p_i] \tag{6}$$

where, p_i is given by Eq. (5) and $F(x_i;\theta)$ represents the one of the three extreme value distributions : the Gumbel, Weibull and Frechet distribution, with parameter vector, θ. The weight W_i is given by following equation. $(k-j+1)$ is the number of peaks. It is based on the concept of tail equivalence(3,10).

$$W_i = \frac{1}{(1-p_i)^2} \tag{7}$$

From the known extreme distribution, the thermal loading parameters, x_k with return periods of k years from the hourly data can be calculated by Eqs. (8) and (9) to follow. The results as well as the optimal estimates of $\tilde{\alpha}, \tilde{\beta}, \tilde{\lambda}, \tilde{\delta}$, and $\tilde{\gamma}$ for each of the distributions are represented in Table 1. It should be noted

Table. 1 Thermal loading parameters corresponding to various return periods

Thermal loading parameters	Return period (years)			
	1	30	50	100
T_e for maxima,℃ ($\tilde{\alpha}$=28.62, $\tilde{\beta}$=1.222)	39.5	43.6	44.3	45.1
T_e for minima,℃ ($\tilde{\alpha}$=11.49, $\tilde{\beta}$=2.034)	-6.6	-13.5	-14.6	-16.0
ΔT_v for maxima,℃ ($\tilde{\alpha}$=2.155, $\tilde{\beta}$=0.6609)	8.0	10.3	10.6	11.1
ΔT_h for maxima,℃ ($\tilde{\lambda}$=3.477, $\tilde{\gamma}$=2.037, $\tilde{\delta}$=21.92)	3.2	3.4	3.4	3.4
$\sigma_{s,\max}$ for maxima, MPa ($\tilde{\lambda}$=18.56, $\tilde{\gamma}$=1.548, $\tilde{\delta}$=136.4)	18.1	18.5	18.5	18.5
$\sigma_{s,\min}$ for minima, MPa ($\tilde{\lambda}$=-46.28, $\tilde{\gamma}$=1.275, $\tilde{\delta}$=977.15)	-45.4	-46.2	-46.2	-46.3

that the return periods in number of years require consideration of the number of hourly data per year (i.e., 7304)

$$x_k = \tilde{\alpha} + \tilde{\beta}\ln(7304k)$$

(Gumbel cdf for maxima) (8a)

$$x_k = \tilde{\alpha} - \tilde{\beta}\ln(7304k)$$

(Gumbel cdf for minima) (8b)

$$x_k = \tilde{\lambda} - \tilde{\delta}(7304k)^{-1/\tilde{\gamma}}$$

(Weibull cdf for maxima) (9a)

$$x_k = \tilde{\lambda} + \tilde{\delta}(7304k)^{-1/\tilde{\gamma}}$$

(Weibull cdf for minima) (9b)

5. Comparison With Current Design Code

The minimum requirements for the design of bridge in Korea are governed by the Highway Bridge Standard Design Specification(12). The code provides for variations in the mean temperature of bridges as well as for temperature differentials between the concrete slab and steel girder. It is suggested in the specification that variation of +50℃ and -10℃ for moderate and +50℃ and -30℃ for cold climate condition is used to calculate thermal expansion and contraction of a composite bridge superstructure. Temperature difference of 10℃ in a cross section between concrete slab and steel girder due to unequal heating (or cooling), is also suggested for the design of composite bridges as shown in Fig. 8. The heating phase is when the concrete slab is at a higher temperature than the steel girder and the cooling phase when the steel girder is at a higher temperature than the concrete slab.

The 1 in 50 year value of maximum effective temperature in Table 1 is only 44.27℃ in contrast to suggested design values of 50℃. Conversely, the current specification suggests a higher value for minimum effective temperature compared with the calculated value shown in Table 1 by about 6℃. If a 1 in 50 year value is taken as the design value, it may be appropriate for design effective temperature of a composite bridge located in moderate climate region to be modified in the range of temperature from -10℃~50℃ to -15℃~45℃.

For the differential temperature and self-equilibrated stresses defined in Eqs. (2) and (3), the design specification for temperature profile shown in Fig. 8 is not strictly comparable with the results of statistical analysis of measured temperature data.

Therefore, it is worthwhile calculating the temperature difference and thermal restraint stresses induced by the uniform

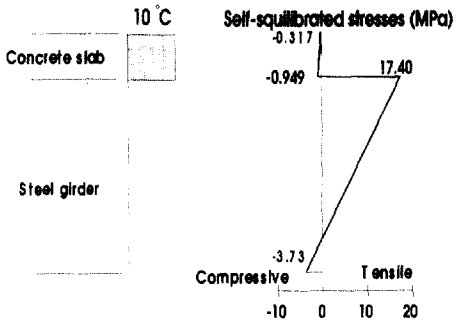

Fig. 8 Current design temperature and self-equilibrated stress profile

temperature distribution of current specification in the previously defined cross section. Thus, the current design temperature distribution has been processed to yield the linear temperature difference and the self-equilibrated stress profile which is illustrated in Fig. 8.

In the figure, the temperature profile in heating phase results in stress distributions with a compressive zone in the lower fibers of the web and a tensile zone in the upper fibers of the web. Regarding the stress profile in cooling phase, the tensile and compressive zones are reversed.

The structural steel in the interface zone of the cross section using the current design temperature distribution is subjected to maximum tensile thermal stress of 17.4MPa as shown in Fig. 8 which is similar to the estimated value of 18.5MPa corresponding to 50-year return period from the statistical analysis(see Table 1). On the other hand, there is a considerable difference between the maximum compressive stress of -17.4MPa which occurs in the interface zone under the cooling phase of the current design temperature difference with -46.2MPa corresponding to 50-year return period which occurs in the vicinity of the bottom third of the south-face web.

The magnitude of the equivalent linear temperature difference of 10.52℃ induced by the design temperature distribution proposed in the current specification is approximately equal to the 1 in 50 year value of 10.6℃ estimated from the statistical analysis of measured data (see Table 1).

There is no suggestion on the horizontal temperature differentials in the current specification. In particular cases however, a horizontal temperature difference may need to be considered. From the result of the statistical analysis, 4℃ should be taken as the temperature difference to be used in design of bridge with a web to be exposed to direct solar radiation.

6. Conclusions

It has been argued that the environmental condition upon which temperature profile in bridge depends exhibits variation with successive years as well as days and seasons, therefore design criteria for temperature effects in bridges should be determined using a probabilistic approach. In this paper, these effects have been considered with the long-term measured temperature in a composite box girder bridge.

As noted before, a closer look at the peak values of hourly data of thermal loading parameters which are previously defined reveals some interesting patterns as follows:

(i) The extreme peaks of T_e for maxima and minima and the extreme ambient air temperatures occur just on the same days, respectively. This specifies the extreme effective temperature range solely on the basis of extreme daily maxima or minima temperatures, regardless of the solar

radiation.

(ii) It is also interesting that the transverse temperature difference is no longer negligible. It is of the same order of magnitude as the vertical temperature difference in some cases. It is chiefly governed by intense solar radiation subjected to a lateral web, therefore the extreme values occurred in days of winter month with lower solar altitude.

(iii) The lateral south-facing web of the box girder exposed to direct solar radiation undergoes a sizable temperature increase almost instantly, so that the zone of the lateral surface exposed to direct solar radiation is subjected to a large compressive stresses of a magnitude of -45.38MPa during the period of measurement. These stresses generally occurred not in days of summer months, but in sunny days of winter months with lower solar altitude.

Additionally, statistical analysis for the measured temperature data is conducted to be willing to extrapolate values with return periods more than that of measurement itself. The results are compared with the specifications suggested in a current design code for thermal loads.

(i) Comparing with the 1 in 50 year value of effective temperature, it may be appropriate to be modified in the range of temperature from -10℃~50℃ to -15℃~45℃. And the vertical temperature difference proposed in the current specification is approximately equal to the 1 in 50 year value.

(ii) There is no suggestion on the horizontal temperature differentials in the current specification. From the result of the statistical analysis, 4℃ should be taken as the temperature difference to be used in design of bridge with a web to be exposed to direct solar radiation.

(iii) The current design code is unsuitable for representing the compressive self-equilibrated thermal stresses in composite bridges. An emphasis should be placed on the magnitude of the compressive self-equilibrated thermal stresses in the lateral web exposed to direct solar radiation.

감사의 말

본 논문은 POSCO 석좌교수연구기금의 지원을 받아 수행된 것이며, 이에 감사의 뜻을 표합니다.

Refernces

(1) Hirst, M.J.S., 1988, Thermal Loading of South Australian Bridges, Australian Road Research Board Internal Report, AIR 420-1.

(2) Ho, D. and Liu, C.H., 1989, Extreme thermal loadings in highway bridges, Journal of Structural Engineering, Vol. 115, No. 7, pp. 1681-1696.

(3) Maes, M.A., Dilger, W.H. and Ballyk, P.D., 1992, Extreme values of thermal loading parameters in concrete bridges, Canadian Journal of Civil Engineering, vol. 19, pp. 935-946.

(4) Maes, M.A., 1989, The extremes of combinations of environmental loads, 5th International Conference on Structural Safety and Reliability, pp.

1823-1826.
(5) Fridley, K.J., Roberts, K.A. and Mitchell, J.B., 1994, Estimating ground snow loads using local crimatological data, Journal of Structural Engineering, Vol. 120, No. 12, pp. 3567-3576.
(6) Dilger, W.H., Beauchamp, J.C., Cheung, M.S. and Ghali, A., 1981, Field Measurements of Muskwa River Bridge, Journal of the Structural Division, Vol. 107, No. ST11, pp. 2147-2161.
(7) Dilger, W.H., Ghali, A., Cheung, M.S. and Maes, M.A., 1983, Temperature Stresses in Composite Box Girder Bridges, Journal of Structural Engineering, Vol. 109, No. 6, pp. 1460-1478.
(8) Mirambell, E. and Costa, J., 1997, Thermal Stresses in Composite Bridges According to BS5400 and EC1, Proceedings of the Institution of Civil Engineers: Structures & Buildings, Vol. 122, Aug., pp. 281-292.
(9) Resnick, S.I., 1971, Tail Equivalence and Its Applications, Journal of Applied Probability, Vol. 8, pp. 135-156.
(10) Castillo, M., 1988, Extreme Value Theory in Engineering, Academic Press Inc., Boston.
(11) Kuester, J.L. and Mize, J.H., 1973, Optimization Techniques with FORTRAN, McGraw-Hill, New York., Chapter 10.
(12) Highway Bridge Standard Design Specification (도로교 표준시방서), 1996, Korean Society of Civil Engineers (사단법인 대한토목학회)

(접수일자 : 1998년 8월 7일)